

## Chapter 2

# Renewable Energy Sources and Energy Conversion Devices

Renewable energy sources are those sources that are regenerative or can provide energy, for all practical purposes, indefinitely. These include solar, wind, geothermal, tidal, wave, hydropower and biomass. The status of development, installed capacity, theoretical potential and other considerations are shown in Table 2.1 on the next page.

### 2.1 Solar Energy

The information contained in this section is based on Duffie and Beckman's Solar Engineering of Thermal Processes, 2nd Edn [8]. For a more comprehensive treatment of the subject of solar engineering and calculations, please refer to the above referenced book.

#### 2.1.1 The Solar Constant

The sun provides energy to the earth in the form of radiation. The radiation emitted by the sun and its spatial relationship to the earth result in a nearly constant intensity of solar radiation at the outer edge of the earth's atmosphere. The amount of energy received by the earth per unit time, based on the average distance between the sun and the earth over the period of a year, is known as the global solar constant,  $G_{sc}$ . The generally accepted value of the global solar constant is  $1367 \text{ W/m}^2$  ( $433 \text{ Btu/ft}^2 \text{ h}$ ,  $4.92 \text{ MJ/m}^2 \text{ h}$ ) with an uncertainty of  $\sim 1\%$ . This value can be used to calculate several values of interest when performing solar calculations.

**Table 2.1** Renewable energy resources: status, installed and potential capacity, and environmental, social and aesthetic considerations

	Status of technology	Installed capacity (GW)	Theoretical potential (GW)	Environmental considerations	Aesthetic/social considerations
Solar (Electricity)	Commercial	5.3 (2005) [1]	~82,000		– Land area use
Solar (Thermal)	Commercial	70 (2004) [1]	~82,000		– Land area use
	Commercial	~59 (2005) [2]	2900–7200 [3]	– Low impact on wildlife – Impact on sensitive species possible – Low impact on aquatic species (offshore/near-shore) – CO <sub>2</sub> , hydrogen sulfide and mercury emissions – Same as geothermal (electrical)	– Noisy – Visually intrusive
Geothermal (Electricity)	Commercial	7.7 (2001) [4]	NA		NA
Geothermal (Thermal)	Commercial	16.7 (2001) [4]	NA		NA
Tidal	Under development	NA	87.4 [5]	– Estuary impact (e.g. sedimentation change) – Impact on migratory fish and birds	NA
Wave	Under development	NA	NA	NA	NA
Hydropower	Commercial	692 (2001) [6]	~2100 [6]	– May disturb aquatic ecosystems – Changes in sedimentation – Incomplete combustion leads to emission of pollutants	– Displacement of people – Loss of culture – Fuel wood collection burdensome on women and children
Biomass (including Wood)	Under development	NA	~41,000		

### 2.1.2 Variation of Extraterrestrial Radiation

Variation in the distance between the earth and the sun during the year leads to variations in extraterrestrial radiation of as much as  $\pm 3\%$ . The dependence of extraterrestrial radiation on time of year is given by Eq. 2.1.

$$G_{en} = G_{sc} \left( 1 + 0.033 \cos \frac{360n}{365} \right) \quad (2.1)$$

where  $G_{en}$  is the extraterrestrial radiation measured on the plane normal to the radiation on the  $n$ th day of the year.

The demand for energy is projected to increase to 30 TW by 2050 and 46 TW by 2100 [7]. The earth's solar resource is more than sufficient to meet this demand and the technology to harness this energy is mature enough for deployment, although improvement in the economics is necessary for wide spread adoption.

The wind energy resource can make a significant contribution to energy demand in the near term, is technologically mature and economically attractive. Of the other resources listed, they do not possess sufficient exploitable capacity to meet demand or they are not technologically mature enough for deployment in the short-term. For these reasons, solar and wind energy are the primary focus of this book.

### 2.1.3 Extraterrestrial Radiation on a Horizontal Surface

To design energy systems that utilize solar radiation, it is often useful to have a means of determining the theoretical solar radiation at the outer edge of earth's atmosphere. The solar radiation incident on a horizontal plane at the outer edge of earth's atmosphere is given by Eq. 2.2.

$$G_0 = G_{sc} \left( 1 + 0.033 \cos \frac{360n}{365} \right) (\cos \phi \cos \delta \cos \omega + \sin \phi \sin \delta) \quad (2.2)$$

where  $n$  is the day of the year,  $\phi$  is the latitude,  $\delta$  is the declination angle, which is the angular position of the sun at solar noon with respect to the plane of the equator, and  $\omega$  is the hour angle, which is the angular displacement of the sun with respect to the local meridian due to the earth's rotation. Solar noon is time of day when the sun appears the highest in the sky compared to its positions during the rest of the day.

To determine the daily solar radiation on a horizontal surface,  $H_0$ , Eq. 2.2 can be integrated from sunrise to sunset to determine the energy per unit area receive by that surface. The result of this integration is Eq. 2.3.

$$H_0 = \frac{24 \cdot 3600 G_{sc}}{\pi} \left( 1 + 0.033 \cos \frac{360n}{365} \right) \left( \cos \phi \cos \delta \sin \omega_s \frac{\pi \omega_s}{180} \sin \phi \sin \delta \right) \quad (2.3)$$

where  $\omega_s$  is the sunset hour angle. The sunset hour angle can be determined from Eq. 2.4.

$$\cos \omega_s = -\tan \phi \tan \delta \quad (2.4)$$

Similarly, to determine the hourly solar radiation,  $I_0$ , Eq. 2.5 may be used.

$$I_0 = \frac{12 * 3600}{\pi} G_{sc} \left( 1 + 0.033 \cos \frac{360n}{365} \right) * \left[ \cos \phi \cos \delta (\sin \omega_2 - \sin \omega_1) + \frac{\pi(\omega_2 - \omega_1)}{180} \sin \phi \sin \delta \right] \quad (2.5)$$

### 2.1.4 Atmospheric Attenuation of Solar Radiation

Solar radiation interacts with the earth's atmosphere in several ways. It may be: (1) reflected back into space, (2) absorbed by gases and particulates in the atmosphere, (3) transmitted directly to the earth's surface or (4) scattered in the atmosphere.

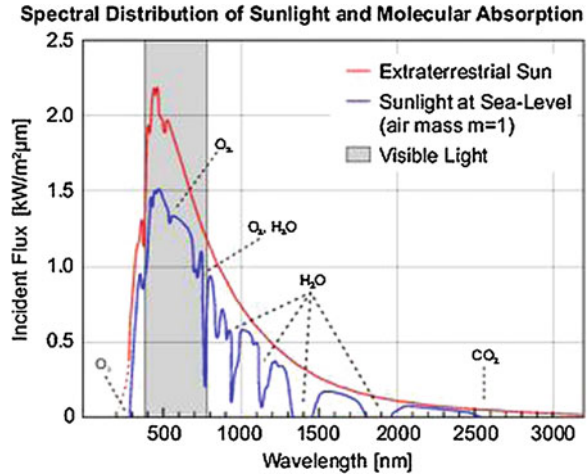
The fraction of radiation reflected back into space is called the albedo and has an annual, latitude-longitude average of 0.35. The reflection is due to reflection from (1) clouds, (2) atmospheric particles and gases and (3) the earth's surface. (4)

The radiation absorbed by the atmosphere causes the warming of the atmosphere. The type and quantity of gases in the atmosphere lead to the attenuation of particular portions of the solar spectrum so that the spectrum at the earth's surface is quite different from that at the outer edge of the atmosphere. X-rays and other very short-wave radiation of the solar spectrum are absorbed by nitrogen and oxygen. Ultraviolet radiation is mainly absorbed by ozone and infrared radiation is mainly absorbed by water vapor and carbon dioxide. After absorption, the resultant wavelength of the spectrum that arrives at the earth's surface is between 0.29 and 2.5  $\mu\text{m}$  (Fig. 2.1).

The radiation can be transmitted directly to the earth's surface or scattered in the atmosphere. Scattering occurs as radiation passes through the atmosphere and interacts with air, water and particulates. The extent of scattering is a function of the degree of particle interactions and the particle size with respect to the wavelength of the radiation. The radiation that is transmitted directly to earth's surface is called direct or beam radiation and the radiation that is scattered is called diffuse radiation. They constitute the radiation that is received by the earth's surface and is used by in solar energy systems.

In summary, the amount of solar radiation available at the earth's surface is a function of time, location (latitude) and also attenuation effects of the earth's atmosphere.

**Fig. 2.1** Spectral distribution of extraterrestrial sunlight and sunlight at sea-level [9]



### 2.1.5 Estimating Monthly Average Solar Radiation

In cases when solar radiation data are not available for a particular location, it is possible to use empirical relationships to estimate radiation values from hours of bright sunshine per day. Equation 2.6 can be used to determine the monthly average daily radiation on a horizontal surface.

$$\frac{\bar{H}}{\bar{H}_0} = a + b \frac{\bar{n}}{\bar{N}} \quad (2.6)$$

where  $\bar{H}$  is the monthly average daily radiation on a horizontal surface,  $\bar{H}_0$  is the extraterrestrial radiation for the location of interested,  $a$  and  $b$  are constants that depend on location,  $\bar{n}$  is the monthly average daily hours of bright sunshine and  $\bar{N}$  is the monthly average number of daylight hours.  $\bar{H}_0$  can be calculated from Eq. 2.3.  $\bar{N}$  can be calculated from Eq. 2.7 shown below by using the mean day of the month to calculate the declination angle,  $\delta$ . The mean day for each month is shown in Table 2.2.

$$N = \frac{2}{15} \cos^{-1}(-\tan \phi \tan \delta) \quad (2.7)$$

Values for  $a$  and  $b$ , the climatic constants, are based on regression analysis of solar radiation data for several geographical locations.

### 2.1.6 Beam and Diffuse Components of Monthly Radiation

Radiation received at the earth's surface can be split into diffuse and beam radiation. Knowledge of these components is important for calculating the incident

**Table 2.2** Average days for months and value for day of year

Month	$n$ for the $i$ th day of month	For the average day of the month	
		Date	$n$ , Day of year
January	$i$	17	17
February	$21 + i$	16	47
March	$59 + i$	16	75
April	$90 + i$	15	105
May	$120 + i$	15	135
June	$151 + i$	11	162
July	$181 + i$	17	198
August	$212 + i$	16	228
September	$243 + i$	15	258
October	$273 + i$	15	288
November	$304 + i$	14	318
December	$334 + i$	10	344

radiation on surfaces that have an orientation that differs from those surfaces for which data is available. It is also important to know the beam component of the total radiation to determine the long-term performance of concentrating solar collectors.

Erbs et al. developed monthly average correlations for the diffuse portion of solar radiation [10]. The correlation is dependent on the monthly average clearness index,  $\bar{K}_T$ , which is defined as  $\bar{H}/\bar{H}_0$ . The equations for the correlation are shown below.  $\bar{H}_d$  is the monthly average diffuse component of radiation:

For  $\omega_S \leq 81.4^\circ$  and  $0.3 \leq \bar{K}_T \leq 0.8$

$$\frac{\bar{H}_d}{\bar{H}} = 1.391 - 3.560\bar{K}_T + 4.189\bar{K}_T^2 - 2.137\bar{K}_T^3 \quad (2.8)$$

and for  $\omega_S > 81.4^\circ$  and  $0.3 \leq \bar{K}_T \leq 0.8$

$$\frac{\bar{H}_d}{\bar{H}} = 1.311 - 3.022\bar{K}_T + 43.427\bar{K}_T^2 - 1.821\bar{K}_T^3 \quad (2.9)$$

### 2.1.7 Radiation on Sloped Surfaces

To determine the radiation on sloped surfaces when only the total radiation is known, the directions from which the diffuse and beam components reach the surface being studied must be determined.

The solar radiation models for determining incident radiation on a sloped surface are based on measured global irradiance on a horizontal surface. On a clear day, the diffuse radiation is composed of three parts: the isotropic component, which is received uniformly from the entire sky dome; the circumsolar diffuse

component, which results from scattering of solar radiation and is concentrated in the area of the sky around the sun; and the horizon brightening component, which is concentrated near the horizon and is apparent in clear skies. The differences among the solar radiation models are in the way they treat the three parts of the diffuse radiation.

The total incident radiation on a sloped surface can be determined using Eq. 2.10.

$$I_T = I_b R_b + I_{d,iso} F_{c-s} + I_{d,cs} R_b + I_{d,hz} F_{c-hz} + I \rho_g F_{c-g} \quad (2.10)$$

$I_b$  is the incident beam radiation on the tilted surface.  $R_b$  is ratio of beam radiation on a tilted plane to that on the plane of measurement and can be calculated using Eq. 2.11.  $I_{d,iso}$  is the incident diffuse radiation due to isotropic part of the diffuse radiation,  $F_{c-s}$  is the view factor of the tilted surface to the sky,  $I_{d,hz}$  is diffuse radiation due to horizon brightening,  $F_{c-hz}$  is the view factor of the tilted surface to the horizon,  $I$  is the total radiation incident on a horizontal surface,  $\rho_g$  is the ground reflectance and  $F_{c-g}$  is the view factor of the tilted surface to the ground.

$$R_b = \frac{\cos \theta}{\cos \theta_z} \quad (2.11)$$

$\theta$  is called the angle of incidence and is the angle between the beam radiation on a surface and the normal to that surface.  $\theta_z$  is called the zenith angle and is the angle of incidence of beam radiation on a horizontal surface.

Equations 2.12 and 2.13 are helpful relationships for determining the values of  $\theta$  and  $\theta_z$ , respectively.

$$\begin{aligned} \cos \theta = & \sin \delta \sin \phi \cos \beta - \sin \delta \cos \phi \sin \beta \cos \gamma \\ & + \cos \delta \cos \phi \cos \beta \cos \omega + \cos \delta \sin \phi \sin \beta \cos \gamma \cos \omega \\ & + \cos \delta \sin \beta \sin \gamma \sin \omega \end{aligned} \quad (2.12)$$

$\beta$  is called the sloped and is the angle between the surface of interest and the horizontal plane.  $\gamma$  is called the surface azimuth angle and is the angular deviation from the local meridian of the projection on a horizontal plane of the normal to the surface.  $\omega$  is called the hour angle and is the angle of the sun east or west of the local meridian.

$$\cos \theta = \cos \theta_z \cos \beta + \sin \theta_z \sin \beta \cos(\gamma_s - \gamma) \quad (2.13)$$

$\gamma_s$  is called the solar azimuth angle and is the angle between the projection of the beam radiation on the horizontal plane and south. It can be determined using Eq. 2.14 through Eq. 2.16.

$$\gamma_s = C_1 C_2 \gamma'_s + C_3 \left( \frac{1 - C_1 C_2}{2} \right) 180 \quad (2.14)$$

$$\sin \gamma'_s = \frac{\sin \omega \cos \delta}{\sin \theta_z} \quad (2.15)$$

$$\begin{aligned} C_1 &= 1 && \text{if } |\omega| \leq \omega_{ew} && \text{or } -1 && \text{if } |\omega| \geq \omega_{ew} \\ C_2 &= 1 && \text{if } |\phi - \delta| \geq 0 && \text{or } -1 && \text{if } |\phi - \delta| \leq 0 \\ C_3 &= 1 && \text{if } \omega \geq 0 && \text{or } -1 && \text{if } \omega \leq 0 \end{aligned}$$

$$\cos \omega_{ew} = \frac{\tan \delta}{\tan \phi} \quad (2.16)$$

$\omega_{ew}$  is the hour angle when the sun is due east or west.

The solar radiation on tilted surfaces can be determined with using several different solar radiation models using measured data for a horizontal surface. The three models described in this section are:

1. Isotropic diffuse model I
2. Hay and Davies model
3. HDKR model

### 2.1.8 The Isotropic Diffuse Model I

The Isotropic Diffuse Model, derived by Liu and Jordan, includes three components to determine the total irradiance: beam, isotropic diffuse and ground reflectance. The third and fourth terms from Eq. 2.10 are considered to be zero since all diffuse radiation is assumed to be isotropic.  $F_{c-s}$  is given by  $(1 + \cos \beta)/2$ .  $F_{c-g}$  is given by  $(1 - \cos \beta)/2$ . Equation 2.10 becomes Eq. 2.17.

$$I_T = I_b R_b + I_d \left( \frac{1 + \cos \beta}{2} \right) + I \rho_g \left( \frac{1 - \cos \beta}{2} \right) \quad (2.17)$$

### 2.1.9 The Hay and Davies Model

The Hay and Davies model differs from the isotropic model in that it provides an estimate of the fraction of diffuse radiation that is circumsolar and assumes that it is from the same direction as the beam radiation. Therefore, the third term in Eq. 2.10 is not zero. The diffuse radiation on the tilted surface is given by Eq. 2.18.

$$I_{d,T} = I_d \left[ (1 - A_i) \left( \frac{1 + \cos \beta}{2} \right) + A_i R_b \right] \quad (2.18)$$



$A_i$  is called the anisotropy index and is defined by Eq. 2.19.

$$A_i = \frac{I_b}{I_0} \quad (2.19)$$

Equation 2.10 then becomes Eq. 2.20.

$$I_T = (I_b + I_d A_i) R_b + I_d (1 - A_i) \left( \frac{1 + \cos \beta}{2} \right) + I \rho_g \left( \frac{1 - \cos \beta}{2} \right) \quad (2.20)$$

### 2.1.10 The HDKR Model

The HDKR model is modified form of the Hay and Davies Model. It contains a horizon brightening term. The diffuse radiation on the tilted surface is given by Eq. 2.21.

$$I_{d,T} = I_d \left[ (1 - A_i) \left( \frac{1 + \cos \beta}{2} \right) \left[ 1 + f \sin^3 \left( \frac{\beta}{2} \right) \right] + A_i R_b \right] \quad (2.21)$$

$F$  is defined by Eq. 2.22.

$$f = \sqrt{\frac{I_b}{I}} \quad (2.22)$$

With these modified terms included, Eq. 2.21 becomes Eq. 2.23.

$$I_T = (I_b + I_d A_i) R_b + I_d (1 - A_i) \left( \frac{1 + \cos \beta}{2} \right) \left[ 1 + f \sin^3 \left( \frac{\beta}{2} \right) \right] + I \rho_g \left( \frac{1 - \cos \beta}{2} \right) \quad (2.23)$$

## 2.2 Photovoltaic Cells

Photovoltaic (PV) cells are devices that absorb light and convert this light directly into electricity. A picture of a solar cell is shown in Fig. 2.2. The solar cell has a dark area, which is usually silicon, and thin silver areas. The silicon absorbs the sunlight and a voltage is generated between the front and back of the cell. The thin silver areas are called front contact fingers and are used to create an electrical contact to the front of the cell. The back of the cell is a solid metal layer that reflects light back up through the cell and provides an electrical contact on the back side. Commercially available cells have a 25–30 year lifetime.

Solar cells are strung together in various serial or parallel configurations to achieve desired electrical characteristics and assembled into modules.

**Fig. 2.2** A PV single cell  
[11]



**Fig. 2.3** Mono-crystalline  
PV module [12]

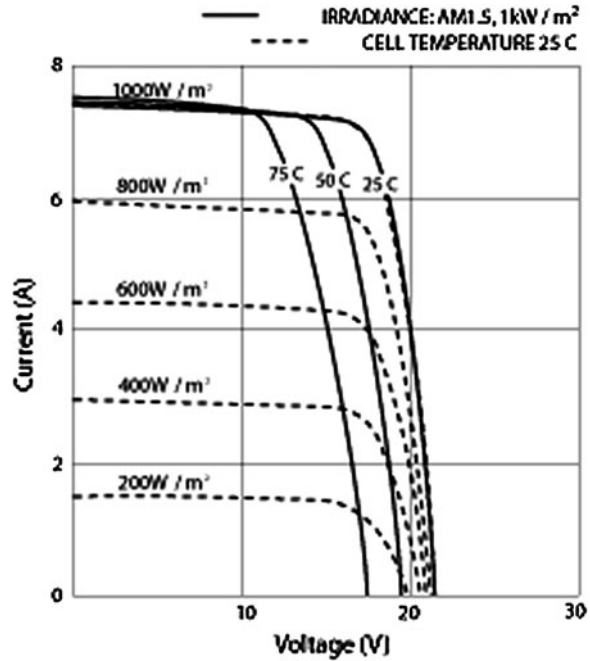


Modules consist of solar cells sealed between two pieces of glass and framed. A picture of PV module is shown in Fig. 2.3. The module protects cells from mechanical damage from handling and the environmental and provides the end user with a robust package that can easily be connected to other modules. A system of connected modules is called an array. The array, in conjunction with electrical conditioning equipment constitutes a complete photovoltaic system. It can be used to meet a user's electrical demand load.

### ***2.2.1 PV Cell Electrical Performance***

Solar cells are characterized by their open-circuit voltage, short-circuit current and I–V (current–voltage) curve. The open-circuit voltage of the cell is the voltage

**Fig. 2.4** I-V curve of PV module under different irradiances and at different temperatures [13]



across the cell when a very high resistance load is connected to the cell. In this case no current is being drawn from the cell. If the load resistance is reduced to zero, the cell is short-circuited and the resultant current in this situation is the short-circuit current. The short-circuit current is directly proportional to the light falling on the cell. The I-V curve is a plot of the current vs. the voltage of the cell as the load is varied. An example of an I-V curve for various ambient temperatures and insolation levels is shown in Fig. 2.4. The power being generated by the solar cell is the product of the voltage and current at any point on the curve. The point on the curve at which the product is greatest is called the maximum power point. The resistance of the load at this point is equal to the cell's internal resistance.

Cell performance is determined under a specified set of standard conditions. Under these conditions, the ambient temperature is 25°C and the power density of the incident solar radiation is 1 kW/m<sup>2</sup> with a spectrum that is equivalent to sunlight that has passed through the atmosphere when the sun is at a 42° elevation from the horizon.

### 2.2.2 Types of PV Cell

There are three main categories of PV cells: (1) inorganic, (2) organic and (3) photoelectrochemical. Of the inorganic type, three sub-types are commercially

available: mono-crystalline, multi-crystalline and amorphous. Mono-crystalline cells are constructed from single crystal silicon ingots by slicing the ingots as is done in microchip fabrication, while multi-crystalline cells are constructed by evaporating coatings onto a substrate. Because grain boundaries exist between crystals in the multi-crystalline cells, electrons can cross at the boundaries which increase losses and reduce efficiency with respect to mono-crystalline cells. Cells using amorphous silicon (a-Si) are of interest because they can be manufactured on continuous lines and require less silicon than the other PV cell types described. The main problem with a-Si cells currently is that they are less efficient than multi-crystalline and mono-crystalline silicon cells. But, because of their lower manufacturing costs, they are able to achieve a lower cost/watt-peak. Typical efficiencies of commercially available PV panels range from 10 to 17%.

### 2.2.3 Inorganic Solar Cell Operation

Photons from the sun can be captured and used directly to produce electricity through the use of a PV cell, which can be made of several semiconductor materials. An explanation of bandgap energy is useful for understanding photon absorption. The bandgap energy is the difference in energy between the top valence band (lower energy) and bottom conduction band (higher energy), as shown in Fig. 2.5. The bands refer to the electron energy ranges for electrons in different electron orbitals. The electrons in the conduction band can be used to create an electrical current. When a photon hits a piece of silicon or another type of semiconductor, several events may occur. If the photon energy is lower than the bandgap energy of the silicon semiconductor, it will pass through the silicon. If the photon energy is greater than the bandgap energy, it will be absorbed.

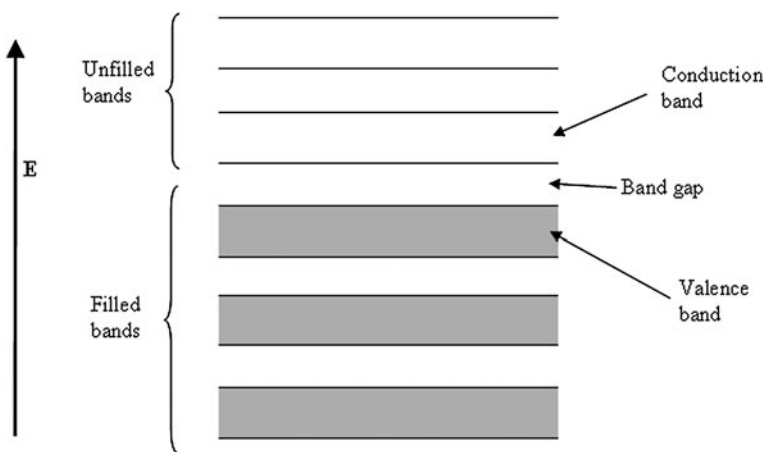


**Fig. 2.5** Schematic of electron bands [14]

When a photon is absorbed, its energy can be given to an electron in the valence band, an electron–hole pair created and heat may be generated. The energy given to the electron excites it and moves it into the conduction band. Now it is free to move around within the semiconductor. The band that the electron was previously a part of now has one less electron. This is known as a hole. The presence of a missing covalent bond allows the bonded electrons of surrounding atoms to move into the hole leaving another hole behind. By this mechanism, a hole can move through the semiconductor opposite the direction that the electrons flow. As a result, moving electrons and holes are created and move to opposite sides of the cell structure. This freedom of movement that occurs as a result of the absorption of the photon is what allows a charge differential (voltage) to be created within the cell. By connecting an external circuit to the two sides of the silicon cell, electrons can recombine with holes and this flow of electrons via this external circuit can be utilized to do work.

To construct an actual cell, an n-type semiconductor (one with excess electrons that can donate electrons) and a p-type semiconductor (one deficient in electrons that can accept electrons) must be placed in physical contact with one another. The semiconductors can be modified by adding impurities, known as dopants, to the Si material. Depending on the number of electrons possessed by the dopant, an n-type or p-type semiconductor can be formed.

### ***2.2.4 Organic Solar Cell Operation***

Organic solar cells also operate with junctions, but the n-type and p-type semiconductors are organic compounds, and the junction between the n- and p-type materials does not produce an electric field. It has a different function than the inorganic p–n junctions. When electrons and holes are produced upon absorption of light, the electrons and holes become bound to one another to form electron–hole pairs called excitons. The excitons have no net electrical charge and cannot carry current. They must be broken apart in order to produce the free electrons and holes required to generate a current. This is the function of the junction between the n- and p-type organic compounds. When the excitons diffuse to this region of the cell, they split apart and produce the required free electrons and holes.

### ***2.2.5 The Current State and Future of Solar Cells***

Solar cell technologies are divided into Generation I, II and III cells. Generation I cells include single-crystal and multi-crystal Si solar cells. Generation II cells include those that involve the use of several types of thin films including both inorganic and organic materials. Generation III cells are denoted by their ability to operate above the 32% thermodynamic efficiency limit known as the

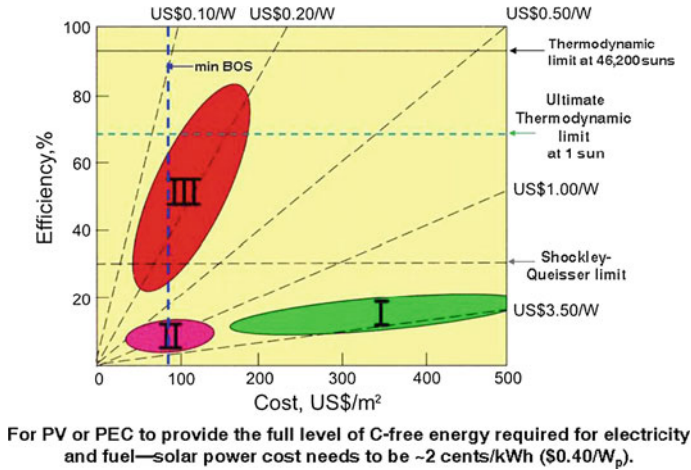


**Fig. 2.6** Cost and efficiency of generation I, II and III PV cells [15]

Shockley-Queisser limit. How is this possible? There are two suggested ways. One assumption made in the original calculations of the above limit is that the energy of an absorbed photon above the bandgap energy becomes heat. If this assumption is not made, the thermodynamic increases to 65%. This can only be accomplished if the material that absorbs the photon is able to utilize the excess photon energy. The other way to accomplish this is through the use of multi-junction cells. Multi-junction cells utilize several materials together with different bandgaps that are able to utilize photons with different energy levels. These cells have been shown to operate at efficiencies higher than those of single-crystal Si cells.

Figure 2.6 shows efficiency plotted against cost (US\$/m<sup>2</sup>) for Generation I, II and III cells. Dashed lines show the cost per W<sub>p</sub> and the Shockley-Queisser limit and thermodynamic limits at 1 sun and 46,200 suns are also shown.

Figure 2.7 shows the efficiency of different PV technologies plotted against time. The different colored lines and tick marks correspond to different PV technologies. The names at each tick mark are the labs or companies that achieved the given efficiency.

### 2.2.6 Solar Concentrators and Trackers

In order to reduce the cost of PV systems, solar concentrators may be utilized. A solar concentrator focuses light on a solar cell at intensities several times higher than that provided by a single sun. Several types of concentrators exist including parabolic, Fresnel and Winston. The benefit of such an approach is that, since the solar cell current is proportional to the intensity of the light incident to the cell, the solar cell should provide a higher current. By substituting inexpensive optics for expensive semiconductor material, system costs are reduced.

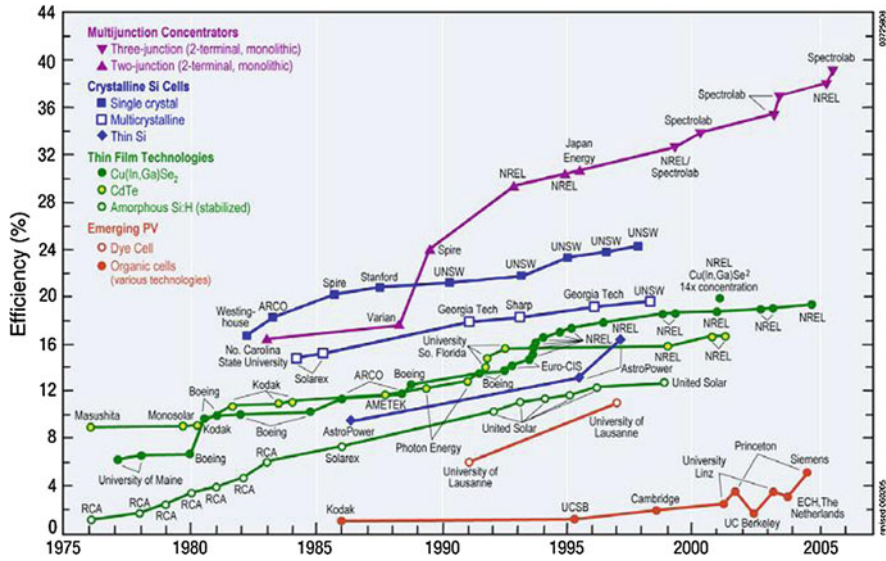


Fig. 2.7 PV efficiencies from 1976 to 2004 [16]

Such a system is not without its problems. First, because of the increased light intensity, the cell begins to overheat and some passive or active means of heat management is required. This will increase costs. Depending on the geographical location of the system, the use of concentrators may not make sense. Additionally, solar cell performance will decrease with an increase in cell temperature.

Second, the typical material used to seal the PV cells between glass, EVA, will degrade at high temperatures. More expensive encapsulation materials, such as silicon, will be required and this too will increase costs.

Lastly, for concentrators to be most effective, a tracker system will be required. Two types of tracking systems exist: single axis and double axis. Single axis systems track the sun as it moves throughout the day (azimuthal tracking). Double axis systems follow both the daily movement of the sun across the sky and the annual change in the sun's position. For a flat-plate collector, which a PV module is, the maximum average gain from using a two axis system (less than a factor of 2) would rarely justify the extra cost of the tracking system, which currently costs more than simply doubling the collector area [17].

### 2.2.7 Economics

Photovoltaic cells incur no fuel expenses, but they do involve a capital cost. The cost for the electricity produced by the cell is determined based on the capital cost of the PV module and the total electrical energy generated over the module's

lifetime. In addition to module costs, a PV system also has costs associated with the power conditioning and energy storage components of the system. These are called balance of system costs, and they are currently in the range of \$250/m<sup>2</sup> for Generation I cells. Therefore, the total cost of present PV systems is about \$6/Wp. A quick rule of thumb to convert the \$/Wp cost figure to \$/kWh follows the relationship: \$1/Wp  $\sim$  \$0.05/kWh. This calculation leads to a present cost for grid-connected (no storage) PV electricity of about \$0.30/kWh.

## **2.3 Wind Energy**

### ***2.3.1 Wind Generation***

Wind is caused by air flowing from high pressure to low pressure regions of the atmosphere. There are two causes for this variation in pressure: (1) the heating of the atmosphere by the sun and (2) the rotation of the earth.

The warming effect of the sun varies with latitude and with the time of day. Warmer air is less dense than cooler air and rises above it so the pressure above the equator is lower than the pressure above the poles. This phenomenon results in a convective current that moves the air higher in the atmosphere at the equator, then toward the poles where the air cools and falls back towards the earth's surface, and finally returns to the equator.

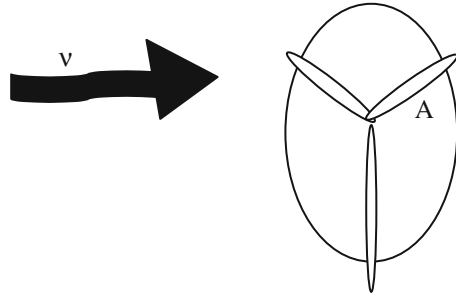
As the earth spins on its axis, it drags the atmosphere with it. The air higher up in the atmosphere is less affected by this drag effect. Instead of traveling in a straight line, the path of the moving air veers to the right. The result of the phenomena described is that the wind circles in a clockwise direction towards the area of low pressure in the Northern hemisphere and counter-clockwise in the Southern hemisphere.

### ***2.3.2 Wind Data Collection and Siting***

Sites that may be attractive to wind development are selected using a wind map and validated with wind measurements. A wind map is constructed using meteorological wind data, which is usually not sufficient to accurately site a large wind power project. After preliminary identification, data collection equipment (anemometer) is used to record the wind speed and direction for several locations at a given site, usually for a year. A higher resolution wind map of the area of interest is then constructed to identify the best location for turbines. This process is known as micro-siting. A good location would have a near constant flow of non-turbulent wind throughout the year without too many sudden bursts of wind.



**Fig. 2.8** Diagram showing air (fluid) with speed,  $v$ , and density,  $\rho$ , moving perpendicular to wind turbine blades with swept area,  $A$



Wind farms often have many turbines installed. Since each turbine extracts some of the energy of the wind, it is important to provide adequate spacing between turbines to prevent interference and reduced energy conversion. As a general rule, turbines are spaced three to five rotor diameters apart perpendicular to the prevailing wind and five to ten rotor diameters apart in the direction of the prevailing wind

The power of the wind passing perpendicularly through a given area, shown in Fig. 2.8, is determined by Eq. 2.24 shown below.

$$P = \frac{1}{2} \rho A v^3 \quad (2.24)$$

where

$P$  = power

$\rho$  = density of the fluid

$A$  = the area through which the fluid is flowing

$v$  = the wind speed

The theoretical maximum amount of energy that can be extracted by a wind turbine was determined to be 59.3% by Albert Betz [18].

### 2.3.3 Wind Turbine Types and Operation

Several types of wind turbine designs exist, though the dominant design is a horizontally-mounted propeller type shown in Fig. 2.9.

These types of turbines typically have two or three blades that are evenly distributed around the axis of rotation. These blades are designed to rotate at a specific angular velocity and torque. The mechanical energy produced can then be further converted to other forms of energy depending on the application (Fig. 2.9).

To convert the mechanical energy to electrical energy, a generator is coupled to the shaft of the propeller. The generator can be designed to operate at a fixed or variable angular velocity. For those generators designed to work at a fixed angular velocity, a transmission will be used to change the angular velocity from that of

**Fig. 2.9** Photo of horizontal axis wind turbine [19]



the propeller to that required by the generator. This type of generator will output the electrical energy as an AC current with constant frequency (usually that of the electrical grid to which it is connected). Alternatively, the energy converter may operate in a variable frequency mode. The electrical energy of this type of system would be output as an AC current with varying frequency [20].

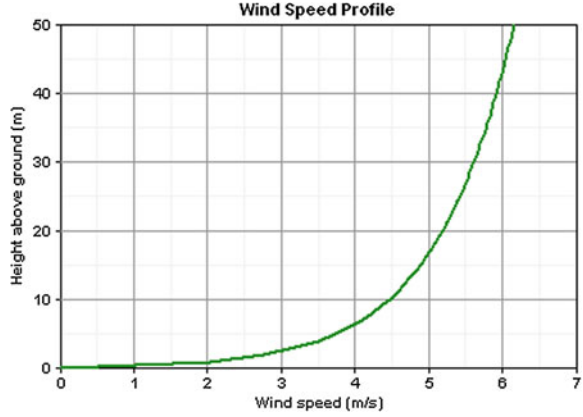
### 2.3.4 Determining Wind Turbine Power Output

To determine the power generated in a particular hour by a given turbine, three calculations are required. First, the wind speed data must be corrected to compensate for the difference between the height of the wind anemometer that was used to collect the wind speed data and the hub height of the turbine being considered in the calculations. The hub height is the height of the turbine as measured from the ground where the turbine is installed to the center of rotation of the turbine blades. The wind speed profile is shown in Fig. 2.10.

A logarithmic or power law relationship can be used to determine the wind speed at the turbine's hub height as shown in Eq. 2.25 and 2.26 respectively.

$$\frac{v(z_{hub})}{v(z_{anem})} = \frac{\ln(z_{hub}/z_0)}{\ln(z_{anem}/z_0)} \quad (2.25)$$

**Fig. 2.10** Logarithmic wind speed profile with surface roughness length = 0.15



where

$v(z_{\text{hub}})$  = wind speed at hub height  
 $v(z_{\text{anem}})$  = wind speed at anemometer height  
 $z_{\text{hub}}$  = hub height of the wind turbine  
 $z_{\text{anem}}$  = height of wind anemometer  
 $z_0$  = surface roughness length

$$\frac{v(z_{\text{hub}})}{v(z_{\text{anem}})} = \left( \frac{z_{\text{hub}}}{z_{\text{anem}}} \right)^{\alpha} \quad (2.26)$$

Where:  $\alpha$  = the power law exponent (Note: Research in fluid mechanics has shown that its value is equal to 1/7 for turbulent flow over a flat plate. Wind speed researchers, however, have found that the exponent depends on temperature, season, terrain roughness, and several other factors.)

Second, a power curve as shown in Fig. 2.11 for the turbine is used to determine the power output of the turbine given the corrected wind speed. The power curve is a plot of the power output for a turbine plotted against wind speed. The turbine shown in this example is a WES18 80 kW turbine [21].

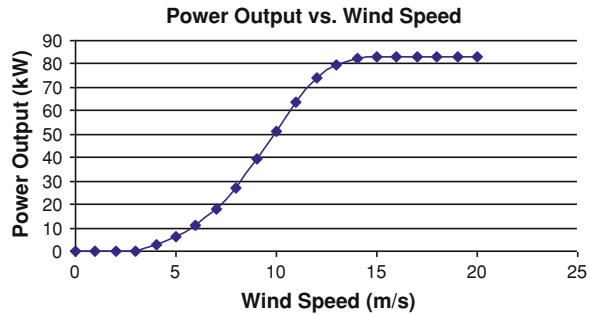
Lastly, the power captured from the wind depends not only on the wind turbine and the wind speed, but also on the air density. Thus, the power output determined above in the second step is multiplied by the air density ratio, which is the air density at the location of interest divided by the air density at standard conditions. This ratio corrects for the altitude of the location of interest and is calculated as shown below in Eq. 2.27.

$$\frac{\rho}{\rho_0} = \left( 1 - \frac{Bz}{T_0} \right)^{\frac{g}{RB}} \left( \frac{T_0}{T_0 - Bz} \right) \quad (2.27)$$

where

$\rho$  = air density ( $\text{kg/m}^3$ )

**Fig. 2.11** Power curve for WES 18 wind turbine [21]



$\rho_0$  = standard air density ( $\text{kg/m}^3$ )

$B$  = lapse rate ( $0.00650 \text{ K/m}$ )

$z$  = altitude (m)

$T_0$  = standard temperature (K)

$g$  = acceleration due to gravity ( $9.81 \text{ m/s}^2$ )

$R$  = gas constant ( $287 \text{ J/kg} \cdot \text{K}$ )

## References

1. Trends in Photovoltaic Applications. International Energy Agency (2006)
2. Wind Energy Association- Statistics." World Wind Energy Association. 6 Mar 2006. World Wind Energy Association. 9 Jan 2007. [http://www.windea.org/home/index.php?option=com\\_content&task=blogcategory&id=21&Itemid=43](http://www.windea.org/home/index.php?option=com_content&task=blogcategory&id=21&Itemid=43)
3. Archer CL, Jacobson MZ (2004) Evaluation of global wind power. J Geophys Res. 9 Jan 2007. [http://www.stanford.edu/group/efmh/winds/global\\_winds.html](http://www.stanford.edu/group/efmh/winds/global_winds.html)
4. Carella R (2001) World energy council survey of energy resources. World Energy Council. 9 Jan 2007. <http://www.worldenergy.org/wec-geis/publications/reports/ser/geo/geo.asp>
5. Craig J (2001) World energy council survey of energy resources. World Energy Council. 9 Jan 2007. <http://www.worldenergy.org/wec-geis/publications/reports/ser/tide/tide.asp>
6. Lafitte R (2001) World energy council survey of energy resources. World Energy Council. 9 Jan 2007. [Craig J (2001) World energy council survey of energy resources. World Energy Council 9 Jan 2007]
7. Nault RM (2005) comp. Basic Research Needs for Solar Energy Utilization. Basic Energy Sciences, U.S. DOE. Argonne National Laboratory, Argonne, IL, 2005. 3. [http://www.sc.doe.gov/bes/reports/files/SEU\\_rpt.pdf](http://www.sc.doe.gov/bes/reports/files/SEU_rpt.pdf)
8. Duffie JA, Beckman WA (1991) Solar energy engineering, 2nd edn. Wiley, London, pp 1–146
9. Digital image [Spectral Distribution of Sunlight]. London Metropolitan University. [http://www.learn.londonmet.ac.uk/packages/clear/visual/daylight/sun\\_sky/images/solar\\_radiation.png](http://www.learn.londonmet.ac.uk/packages/clear/visual/daylight/sun_sky/images/solar_radiation.png)
10. Erbs DG, Klein SA, Duffie JA (1982) Estimation of the diffuse radiation fraction for hourly, daily and monthly-average global radiation. Sol Energy 28:292–302
11. Digital image [Picture of Siemen Cell]. Energy Center of Wisconsin. [http://www.wisconsin.org/images/siemen\\_cell.jpg](http://www.wisconsin.org/images/siemen_cell.jpg)
12. Digital image [Sharp PV Module]. <http://www.hanseatic-trade-company.de/images/sharp-modul.jpg>

13. Digital image [PV Module I-V Curver]. [http://www.kyocerasolar.com/images/SL\\_irradiance.gif](http://www.kyocerasolar.com/images/SL_irradiance.gif)
14. Digital image [Electronic Band Diagram]. [http://en.wikipedia.org/wiki/Image:Electronic\\_band\\_diagram.svg](http://en.wikipedia.org/wiki/Image:Electronic_band_diagram.svg)
15. Nault RM (2005) comp. Basic Research Needs for Solar Energy Utilization. Basic Energy Sciences, U.S. DOE. Argonne National Laboratory, Argonne, IL 2005. 14. [http://www.sc.doe.gov/bes/reports/files/SEU\\_rpt.pdf](http://www.sc.doe.gov/bes/reports/files/SEU_rpt.pdf)
16. Nault RM (2005) comp. Basic Research Needs for Solar Energy Utilization. Basic Energy Sciences, U.S. DOE. Argonne National Laboratory, Argonne, IL, 2005. 18. [http://www.sc.doe.gov/bes/reports/files/SEU\\_rpt.pdf](http://www.sc.doe.gov/bes/reports/files/SEU_rpt.pdf)
17. Sorensen B (2000) Renewable energy, 2nd edn. Academic Press, London, pp 382–385
18. Sorensen B (2000) Renewable energy, 2nd edn. Academic Press, London, p 345
19. Digital image [Large Windmill]. <http://www.leicageosystems.com/news/images/windmill.jpg>
20. Sorensen B (2000) Renewable energy, 2nd edn. Academic Press, London, p 448
21. “Wind Turbine Manufacturer- WES BV.” WES Wind Turbines

Hybrid Hydrogen Systems  
Stationary and Transportation Applications

Al-Hallaj, S.; Kiszynski, K.

2011, X, 134 p., Hardcover

ISBN: 978-1-84628-466-3